Available online at www.sciencedirect.com
SCIENCE DIRECT
Dyes and Pigments 72 (2007) 150–156
DYES and PIGMENTS
www.elsevier.com/locate/dyepig

Fluorescence emission studies of 4-(2-furylmethylene)-2-phenyl-5-oxazolone embedded in polymer thin film and detection of Fe^{3+} ion

Gulsiye Ozturk, Serap Alp*, Kadriye Ertekin

University of Dokuz Eylül, Faculty of Arts and Sciences, Department of Chemistry, 35160, Tinaztepe Campus, Buca, Izmir, Turkey

Received 2 February 2005; received in revised form 26 July 2005; accepted 18 August 2005
Available online 19 October 2005

Abstract

The photophysical and photochemical properties of azlactone derivative 4-(2-furylmethylene)-2-phenyl-5-oxazolone (PFO) were examined in solvents of tetrahydrofuran (THF), acetonitrile (ACN) and dichloromethane (DCM) and in solid matrix of polyvinyl chloride (PVC).

The PFO dye embedded in plasticized PVC matrix has been used in monitoring Fe^{3+}. The PFO dye exhibited satisfactory fluorescence emission based optical response to Fe^{3+} with a detection limit of 3.8×10^{-6} M. The sensor composition exhibited a dynamic response to Fe^{3+} in the concentration range of 6×10^{-6}–6×10^{-4} M. The sensor is fully reversible within the dynamic range and the response time (τ_{90}) is approximately 2 min under batch conditions. The reproducibility of the sensor membrane was investigated by alternately changing the solution of 2×10^{-5} M Fe^{3+} and BES buffer (10^{-3} M, pH = 7.0), and relative standard deviation was calculated as 0.4% ($n = 7$). pH dependence is negligible in the pH range of 4.0–11.0. The cross sensitivity of PFO to Co^{2+}, Ni^{2+}, Zn^{2+} and Cu^{2+} was also tested and evaluated.

Keywords: Fluorescence emission; Azlactone; PVC matrix; Optical sensor; Fe^{3+}

1. Introduction

The continuous determination of heavy metal ions is of growing interest in environmental and clinical analyses [1]. Iron is one of the most important elements among heavy metals for metabolic processes, being indispensable for plants and animals and therefore it is extensively distributed in environmental and biological materials [2].

Widely used analytical techniques for the detection of heavy metals include atomic absorption spectrometry (AAS), inductively coupled plasma emission spectrometry (ICP-ES), total reflection X-ray fluorimetry (TXRF) and anodic stripping voltammetry (ASV). These methods can offer good limits of detection and wide linear ranges, but are very expensive and do not easily lend themselves to miniaturisation [3,4]. The development of sensors based on an immobilized reagent is subject of growing interest [1,3].

In contrast to electrochemical sensors where a close connection of the reagent phase with the electrode body is required, in optical sensors and probes the reagent phase need not be in physical contact with the optoelectronic systems [5].

Capitan-Vallvey et al. [6] developed an optical sensor for determination of iron, which was based on the formation of the Fe^{3+}–ferrozine complex. Even though the method is sensitive it is not reversible.

* Corresponding author. Tel.: +90 232 453 50 72/2255; fax: +90 232 453 41 88.
E-mail address: serap.alp@deu.edu.tr (S. Alp).

0143-7208/$ - see front matter © 2005 Elsevier Ltd. All rights reserved.
doi:10.1016/j.dyepig.2005.08.012

A pH-dependent absorption-based sensor for Fe^{3+} in aqueous media based on the use of 2,4-dinitroresorcinol immobilized on XAD-7 was developed by Malçik and Çaglar [1].

An organic supramolecular compound synthesized from pyrochatechol units was previously used as a stable chelating agent for Fe^{3+} in solution. It was applied as an ionophoric reagent on ion-sensitive field-effect transistor (ISFET) and electrolyte–insulator–semiconductor (EIS) structures and exhibited a detection limit of 10^{-4} M [7].

The literature survey reveals that modified and non-modified atomic spectroscopic techniques are widely used in comparison to other Fe^{3+} determination methods [8–15]. However, a limited number of absorption and emission based optical sensor designs for Fe^{3+} determination exists [16–19]. Thus, we now report the first time usage of the azlactone derivative, 4-(2-furylmethylene)-2-phenyl-5-oxazolone (PFO), for spectrofluorimetric determination of Fe^{3+}.

Azlactone structures have wide range of applications such as their use in semiconductor devices like electrophotographic photoreceptors and in non-linear optical materials, because of their promising photophysical and photochemical activities. In liquid state, the stability of the heterocyclic ring system of the molecule is not satisfactory and fluorescence quantum yields are low. When embedded in a proper polymeric matrix, these structures exhibit higher fluorescence emission and improved stability due to the enhanced molecular rigidity in immobilized phase [20].

Plasticized PVC membranes are believed to be useful for sensor applications because of their good mechanical properties, homogeneity, simplicity of preparation and optical transparency [3].

In this study, the photophysical and photochemical characteristics of PFO in three different solvents and plasticized PVC matrix were determined. The preparation of the fluorescent sensor for Fe^{3+} and its sensor performance characteristics such as response time, dynamic working range, sensitivity and limit of detection were declared. In addition the interferences of various cations and cross sensitivity to pH were also studied.

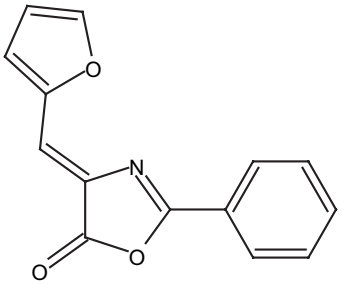

PFO

2. Materials and methods

2.1. Materials

The synthesis and purification of 4-(2-furylmethylene)-2-phenyl-5-oxazolone (PFO) were performed by using general preparation methods of azlactones as described in the literature [21]. The membrane components, PVC (high molecular weight) and the plasticizer bis-(2-ethylhexyl)phthalate (DOP) were supplied by Fluka, lipophilic anionic additive reagent potassium tetrakis-(4-chlorophenyl)borate (PTCPB), tetrahydrofuran (THF), acetonitrile (ACN) and dichloromethane (DCM) were obtained from Aldrich. The buffering agent of *N*,*N*-bis(2-hydroxyethyl)-2-aminoethane sulfonic acid (BES) was purchased from Merck. All other chemicals were obtained from Fluka and Merck. The polyester support (Mylar type) was provided from DuPont, Switzerland. Bidistilled ultrapure water was used throughout the studies.

2.2. Apparatus and spectroscopic measurements

UV–Vis absorption spectra were recorded with Shimadzu UV-1601 spectrophotometer. All fluorescence measurements were performed by using Varian-Cary Eclipse spectrofluorimeter. The pH value of different buffer solutions was adjusted with WTW pH-meter calibrated with Merck pH standards of pH 7.00 (titrisol buffer) and pH 4.01.

Absorption and fluorescence emission spectral data of polymer films were acquired in quartz cells that were filled with sample solution. The polymer films were placed in diagonal position in the quartz cell. The advantage of this kind of a placement was to improve the reproducibility of the measurements.

2.3. Polymer film preparation

A mixture for membrane preparation was obtained by dissolving 120 mg of PVC, 240 mg of plasticizer and stoichiometric amount of PTCPB with PFO in 1.5 mL of dried THF. The concentration of PFO in mixture was about 2 mmol dye/kg polymer. The resulting cocktails were spread onto a 125 μm polyester support (Mylar TM type). The polymer support is optically fully transparent, ion impermeable and exhibits good adhesion to PVC. Sensor slides were kept in a dessicator therefore the damage from the ambient air of laboratory was avoided. Each sensor film was cut to a size of 13×50 mm.

Table 1
UV–Vis absorption maxima, λ_{max} (nm) and molar extinction coefficients, ε ($L\,mol^{-1}\,cm^{-1}$) of PFO in solvents of DCM, ACN, THF and polymer film

Solvent	λ_1	ε_1	λ_2	ε_2
DCM	392	81 000	407[a]	74 000
ACN	387	65 000	400[a]	62 000
THF	389	75 000	405[a]	70 000
PVC film	395	73 883 000	410	68 938 000

[a] The approximate absorption maxima of the shoulders.

3. Results and discussion

3.1. UV–Vis absorption and fluorescence emission spectroscopy studies

The absorption and emission based spectral data are given in Tables 1 and 2. In absorption spectra of 10^{-6} M solutions of PFO, a well-shaped absorption maxima and an accompanying shoulder were observed. The well-defined absorption maxima were at the wavelengths of 392, 389 and 387 nm in the solvents of DCM, THF and ACN, respectively. The absorption maxima of the shoulders that appeared in longer wavelengths were not detectable in the solvents. However, in PVC matrix, the non-detectable shoulders became clear and shifted to longer wavelengths. In comparison to the solution phase, the PVC matrix provided better resolution due to the matrix rigidity (see Fig. 1, Table 1).

In comparison to the solution phase, both absorption maxima of PFO in PVC matrix exhibited red shifts ranging from 3 to 8 nm (Fig. 1, Table 1). These slight red shifts were presumably due to the increase of the polarity of microenvironment of PFO dye. Approximately 1000 fold increase in molar extinction coefficient (ε) of the dye in PVC matrix can be attributed to the enhanced rigidity in immobilized polymer phase.

Emission and related excitation spectra of PFO are presented in Fig. 2. In all of the employed solvents and PVC matrix, the excitation wavelength was chosen as 385 nm and emission spectra were recorded. The excitation spectral data were acquired by exciting the molecule at its emission maximum for each medium. Table 2 summarizes the excitation and emission related data: excitation and emission wavelengths, λ (nm), Stokes' shift values, $\Delta\lambda$ (nm), radiative lifetimes, τ_0 (ns), and singlet energy values, E_s (kcal/mol) of PFO in solutions and plasticized PVC matrix.

Table 2
Excitation and emission wavelengths, λ (nm), Stokes' shift, $\Delta\lambda$ (nm), radiative life time, τ_0 (ns) and singlet energy, E_s (kcal/mol) of PFO in solutions and PVC matrix

Solvent	λ^{f}_{max}	$\Delta\lambda$	λ^{ex}_{max}	τ_0	E_s
DCM	435	43	387	0.0291	72.9
ACN	434	47	385	0.0324	73.8
THF	434	45	385	0.0360	73.4
PVC film	448	53	403	0.3827	72.3

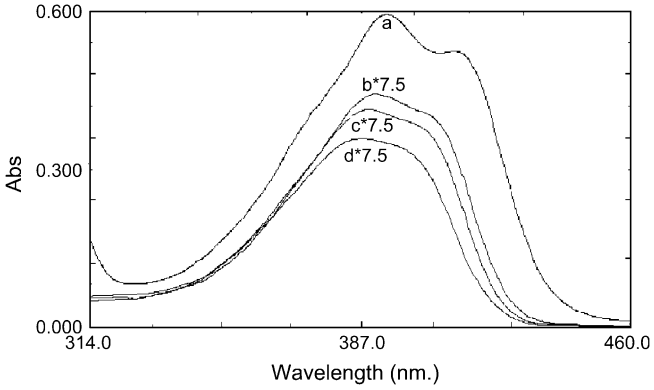

Fig. 1. Absorption spectra of PFO dye in (a) PVC (2 mmol PFO/kg PVC, $\lambda_{max} = 395$ nm), (b) DCM (10^{-6} M PFO, $\lambda_{max} = 392$ nm), (c) THF (10^{-6} M PFO, $\lambda_{max} = 389$ nm) and (d) ACN (10^{-6} M PFO, $\lambda_{max} = 387$ nm).

The PFO dye exhibited moderate results concerning with Stoke' shift values which range from 43 to 53 nm in all of the employed media. The highest Stokes' shift value was observed in PVC matrix, which confers the advantage of better spectral resolution in emission based studies and a desired property in commercially important dyes.

The radiative lifetimes, τ_0, were calculated by the formula $\tau_0 = 3.5 \times 10^8/\nu^2_{max}\varepsilon_{max}\Delta\nu_{1/2}$, where ν_{max} is the wavenumber in cm^{-1}, ε_{max}, the molar absorption coefficient at the selected absorption wavelength, and $\Delta\nu_{1/2}$, the half-width of the selected absorption in wavenumber units of cm^{-1} [20].

Singlet energy of PFO in polymer film matrix, $E_s = 72.3$ kcal/mole, is observed to be slightly lower than that in the solvents. Besides the larger Stokes' shift, having higher radiative lifetime and lower singlet energy

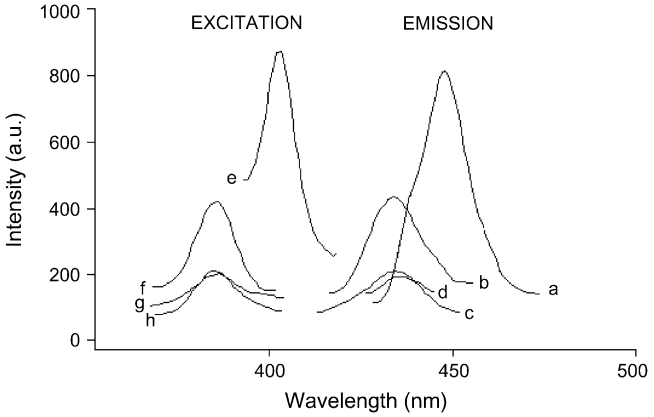

Fig. 2. Emission and excitation spectra of PFO dye in different media when excited at 385 nm. Emission spectra in (a) PVC (2 mmol PFO/kg PVC), (b) THF (10^{-6} M PFO), (c) ACN (10^{-6} M PFO) and (d) DCM (10^{-6} M PFO). Corresponding excitation spectra in (e) PVC, (f) THF, (g) ACN and (h) DCM.

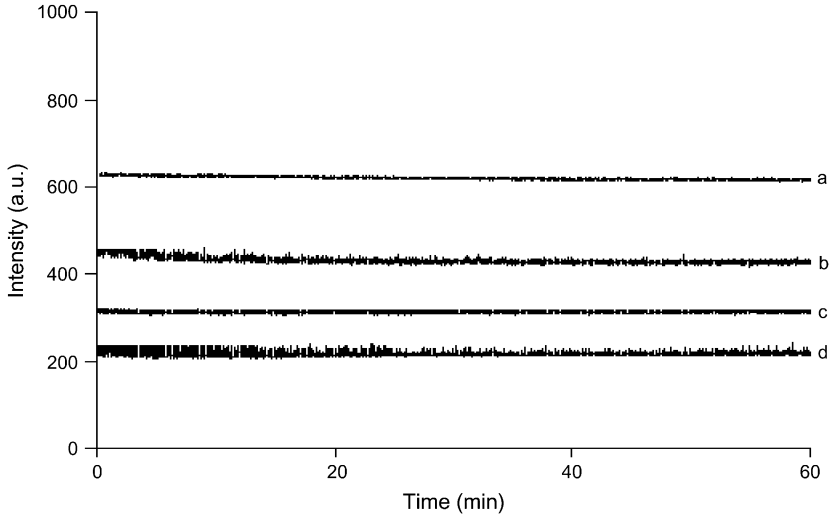

Fig. 3. Photostability test results of PFO in (a) PVC (2 mmol PFO/kg PVC), (b) THF (10^{-6} M PFO), (c) ACN (10^{-6} M PFO) and (d) DCM (10^{-6} M PFO) after 1 h of monitoring.

values are also desirable fluorophore characteristics and enhance the performance of PFO as a sensor molecule.

3.2. Photostability test results

The photostability of azlactone dye in PVC matrix and in solutions of DCM, ACN and THF was monitored and recorded with a steady-state spectrofluorimeter in the mode of time based measurements. The data acquired at 435, 434, 434 and 448 nm correspond to the emission wavelength maximum of PFO in DCM, ACN, THF and PVC, respectively. All of the acquired data were obtained by using the same excitation wavelength of 385 nm. The data collected after 1 h of monitoring are shown in Fig. 3. The experimental results reveal that PFO exhibits excellent photostability in all of the employed solvents and PVC matrix.

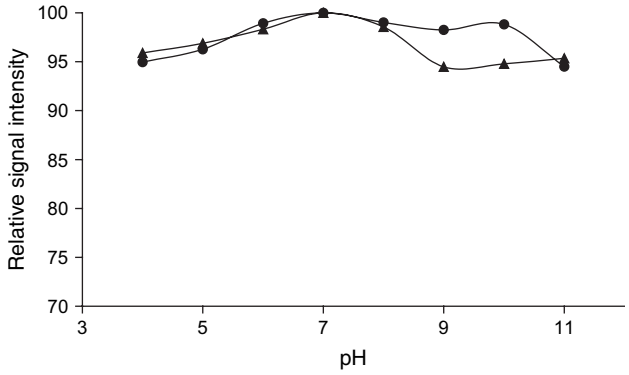

Fig. 4. pH dependence of the fluorescence intensity of PFO (2 mmol PFO/kg PVC) in the pH range of 4.0–11.0. "●" refers to plain buffers (10^{-3} M BES, pH 6.0–8.0; $CH_3COOH/NaCH_3COO$, pH 4.0–5.0; and NH_4Cl/NH_3, pH 9.0–11.0), and "▲" refers to 6×10^{-5} M Fe^{3+} containing buffers.

3.3. Sensing scheme

Electrically neutral polyvinylchloride provides a good solvent medium for uncharged PFO dye. After Fe^{3+} uptake the membrane becomes positively charged. The liphophilic anionic additive reagent, potassium tetrakis-(4-chlorophenyl)borate (PTCPB), behaves as a counter ion and compensates the charge excess. The immobilized PFO dye interacts with Fe^{3+} cations in sample solution via nitrogen belonging to five-membered

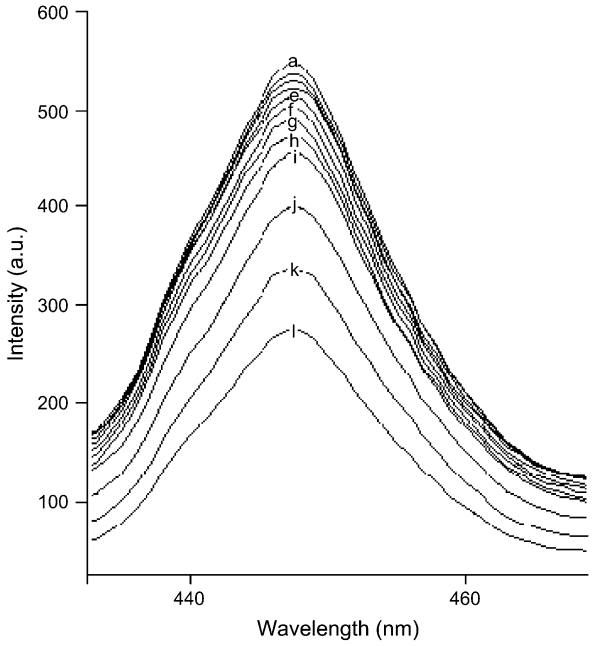

Fig. 5. Emission spectra of immobilized PFO (2 mmol PFO/kg PVC, $\lambda_{ex} = 385$ nm) after exposure to different Fe^{3+} concentrations: (a) 0, (b) 6×10^{-6}, (c) 8×10^{-6}, (d) 1×10^{-5}, (e) 2×10^{-5}, (f) 4×10^{-5}, (g) 6×10^{-5}, (h) 8×10^{-5}, (i) 1×10^{-4}, (j) 2×10^{-4}, (k) 4×10^{-4}, and (l) 6×10^{-4} M.

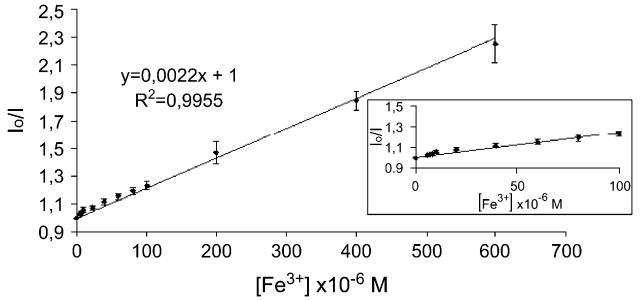

Fig. 6. Calibration plot of sensor in the concentration range of 6×10^{-6}–6×10^{-4} M Fe^{3+} in BES–buffered solutions ($\lambda_{ex} = 385$ nm, 2 mmol PFO/kg PVC).

heteroring and oxygen atom of furyl ring. This interaction is not as strong as a real complexation reaction but is strong enough to bind the Fe^{3+} cations reversibly. Since the polarity of PFO dye has been increased upon excitation, the excited PFO molecule electrostatically interacts with Fe^{3+} and an energy transfer takes place from ligand to metal. The PFO responds to iron by a decrease in fluorescence intensity that has been used as analytical signal.

3.4. Effect of pH on sensor response

The pH dependence of the sensor membrane was investigated both in plain buffers of 10^{-3} M BES (pH 6–8), $CH_3COOH/NaCH_3COO^-$ (pH 4 and 5) and NH_4Cl/NH_3 (pH 9–11), and in the presence of 6×10^{-5} M Fe^{3+} (Fig. 4). Response is slightly affected by pH. Above and below pH 7.00 the signal intensity has shown a slight tendency to decrease. This result indicates that by using the proposed sensor for determination of Fe^{3+}, there is no need for stringent control for the sample solution pH, which simplifies the practical application of the proposed sensor in the determination of Fe^{3+} concentration in real samples.

Although there has been no significant pH dependence in the pH range of 4.0–11.0, the pH of the measurement medium was kept constant at pH 7.0 employing 10^{-3} M BES buffer. At well-defined and constant pH values, the response is reproducible and promising.

3.5. Sensor response to Fe^{3+}

The sensor slides were exposed to BES-buffered Fe^{3+} solutions in the concentration range of 6×10^{-6}–6×10^{-4} M. Fluorescence emission spectra of sensor slides after exposure to Fe^{3+} solutions are shown in Fig. 5.

The normalized (I_o/I) calibration plot of iron sensor in the concentration range of 6×10^{-6}–6×10^{-4} M Fe^{3+} is shown in Fig. 6.

The linearized calibration plot of sensor can be described by $y = 0.0022x + 1$ and the correlation coefficient is 0.9955.

The limit of detection for Fe^{3+} was defined as the concentration at which the signal is equal to the average blank signal ± 3 standard deviation ($n = 20$). The blank signal was taken to be the fluorescence intensity at 478 nm in the absence of Fe^{3+}. The limit of detection (LOD) for Fe^{3+} was found to be 3.8×10^{-6} M.

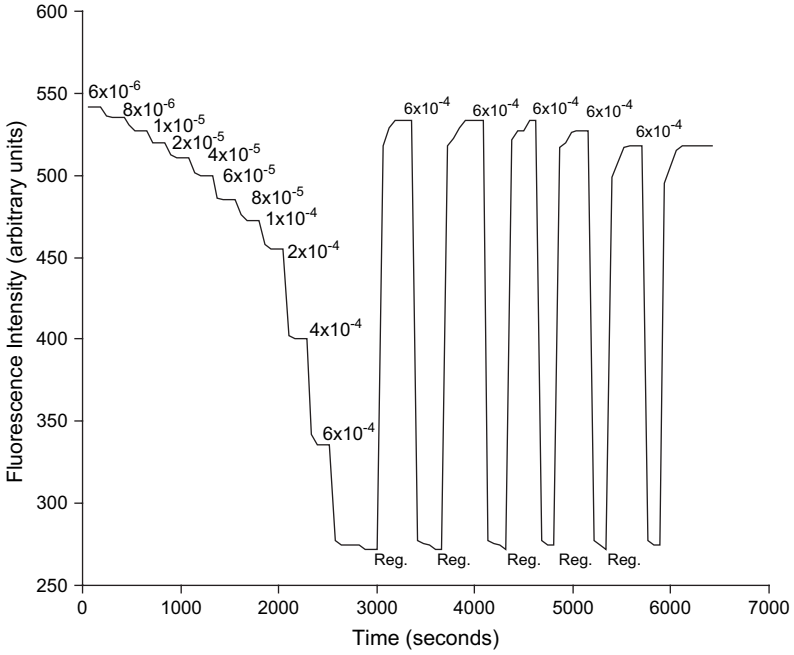

Fig. 7. Intensity based response curve of the sensor slide (2 mmol PFO/kg PVC, $\lambda_{ex} = 385$ nm) in monitoring Fe^{3+} in the concentration range from 6×10^{-6} to 6×10^{-4} M.

Table 3
Effects of interferent cations on the fluorescence signal of the proposed optical sensor (F_1: fluorescence intensity of the sensor membrane in the presence of Fe^{3+} at 4×10^{-5} M, ΔF: difference of fluorescence intensities before and after exposure to interferent cations)

Interferent cations	Concentration (M)	Relative signal change $(\Delta F/F_1) \times 100$
Ni^{2+}	10^{-2}	4.3
Zn^{2+}	10^{-2}	3.8
Co^{2+}	10^{-2}	4.2
Cu^{2+}	10^{-2}	5.6
Cu^{2+}	10^{-3}	5.3

Intensity-based response curve of the sensor membrane to evaluate the reproducibility and reversibility of the sensor is shown in Fig. 7.

By alternately measuring the sample solution with Fe^{3+} concentration of 6×10^{-4} M and regeneration buffer (0.026 mol L^{-1} KH_2PO_4/0.041 mol L^{-1} Na_2HPO_4, pH 7.00), the reproducibility of the membrane was investigated. The relative standard deviation was calculated for upper signal level and found to be 0.4% for seven measurements, which indicates that reproducibility of proposed sensor is satisfactory.

The approximate response time (τ_{90}) was measured as 2 min. The sensor was fully reversible and a positive drift of 1.6% of the upper signal has been observed after the first cycle. The following second and third cycles did not result in any further large drifts. Fluorescence intensity of the dye is found to decrease about 2.7% after the fourth cycle and 4.4% after the fifth and sixth cycles. The results indicate that the reversibility of the proposed sensor is satisfactory.

3.6. Selectivity studies

Interferent effects of cations Co^{2+}, Ni^{2+}, Zn^{2+} and Cu^{2+} were also tested and evaluated. These cations were chosen considering the hydratised ionic radius of iron ($Fe^{3+} = 2.13$, $Co^{2+} = 2.09$, $Ni^{2+} = 2.06$, $Zn^{2+} = 2.17$ and $Cu^{2+} = 2.07$ Å) [22].

By fixing the concentration of Fe^{3+} at 4×10^{-5} M, concentrated solutions of the interfering cations (10^{-2} M), Co^{2+}, Ni^{2+}, Zn^{2+} and Cu^{2+}, were added into the sample solution, and sensor slides were tested to evaluate the selectivity. The relative signal intensity drops caused by the tested possible interferent cations are shown in Table 3.

The interferent effects of cations that caused a relative signal intensity change of less than 5% is negligible. Results in Table 3 reveal that Ni^{2+}, Zn^{2+} and Co^{2+} have negligible interference effect for the determination of Fe^{3+}. The same amount of Cu^{2+} decreased the fluorescence intensity of the PFO by 5.6%. At the concentration of 10^{-3} M of Cu^{2+} the relative signal intensity change becomes smaller, 5.3%.

4. Conclusion

It is proved that the immobilized 4-(2-furylmethylene)-2-phenyl-5-oxazolone (PFO) can be used for Fe^{3+} sensing in the concentration range of 6×10^{-6}–6×10^{-4} M. It has a reproducible response and provides an inexpensive and quick method for the determination of Fe^{3+}. This novel sensor does not require harsh conditions such as an acidic media, thus it has application potential for determination of Fe^{3+}in real samples.

Acknowledgements

Funding for this research was provided by the Scientific Research Funds of Dokuz Eylül University (04 kb Fen 104).

References

[1] Malçik N, Çaglar P. The operational parameters of a new fibre-optic sensor for ferric ions in aqueous media. Sensors and Actuators B 1997;38–39:386–9.
[2] Pulido-Tofino P, Barrero-Moreno JM, Perez-Conde MC. A flow-through sensor to determine Fe(III) and total inorganic iron. Talanta 2000;51:537–45.
[3] Vaughan AA, Narayanaswamy R. Optical fibre reflectance sensors for the detection of heavy metal ions based on immobilized Br-PADAP. Sensors and Actuators B 1998;51:368–76.
[4] Karamanev DG, Nikolov LN, Mamtarkova V. Rapid simultaneous quantitative determination of ferric and ferrous ions in dragine waters and similar solutions. Minerals Engineering 2002;15:341–6.
[5] Oehme I, Wolfbeis OS. Optical sensors for determination of heavy metal ions. Microchimica Acta 1997;126:177–92.
[6] Capitan-Vallvey LF, Arroyo E, Berenguer C, Fernandez-Ramos MD, Avidad R. Single-use optical sensor for the determination of iron in water and white wines. Frensenius' Journal of Analytical Chemistry 2001;369:139–44.
[7] Mlika R, Quada HB, Kalfat R, Gamoudi G, Mhenni F, Jaffrezic-Renault N. Thin sensitive organic membranes on selective iron-ion sensors. Synthetic Metals 1997;90:239–43.
[8] Niemela M, Kola H, Eilola K, Peramaki P. Development of analytical methods for the determination of sub-ppm concentrations of palladium and iron in methorexate. Journal of Pharmaceutical and Biomedical Analysis 2004;35:433–9.
[9] Quaresma MCB, Cassella RJ, Guardia M, Santellia E. Rapid on-line sample dissolution assisted by focused microwave radiation for silicate analysis employing flame atomic absorption spectrometry: iron determination. Talanta 2004;62:807–11.
[10] Yebra MC, Moreno-Cid A, Cespond R, Cancela S. Preparation of a soluble solid sample by a continuous ultrasound assisted dissolution system for the flow-injection atomic absorption spectrometric determination of iron in milk powder and infant formula. Talanta 2004;62:403–6.
[11] Vidal MT, Pascual-Marti MC, Salvador A, Llabata C. Determination of essential methods in complete diet feed by flow injection

and flame atomic absorption spectrometry. Microchemical Journal 2002;72:221–8.
[12] Achterberg EP, Holland TW, Bowie AR, Mantoura RFC, Worsfold PJ. Determination of iron in seawater. Analytica Chimica Acta 2001;442:1–14.
[13] Canfranc E, Abarca A, Sierra I, Marina ML. Determination of iron and molybdenum in a dietetic preparation by flame AAS after dry ashing. Journal of Pharmaceutical and Biomedical Analysis 2001;25:103–8.
[14] Anzaro JM, Gonzalez P. Determination of iron and copper in peanuts by flame atomic absorption spectrometry using acid digestion. Microchemical Journal 2000;64:141–5.
[15] Bermejo P, Pena E, Dominguez R, Bermejo A, Fraga JM, Cocho JA. Speciation of iron in breast milk and infant formulas whey by size exclusion chromatography–high performance liquid chromatography and electrothermal atomic absorption spectrometry. Talanta 2000;50:1211–22.
[16] Ohno S, Teshima N, Zhang H, Sakai T. Utilization of activating and masking effects by ligands for highly selective catalytic spectrophotometric determination of copper and iron in natural waters. Talanta 2003;60:1177–85.
[17] Quinteros A, Farre R, Lagarda MJ. Optimization of iron speciation (soluble, ferrous and ferric) in beans, chickpeas and lentils. Food Chemistry 2001;75:365–70.
[18] Dominik P, Kaupenjohann M. Simple spectrophotometric determination of Fe in oxalate and HCl soil extracts. Talanta 2000;51:701–7.
[19] Tomiyasu T, Yonehara N, Teshima N, Kawashima T. Kinetic method for the determination of iron (II, III) by its catalytic effect on the oxidation of 3-methyl-2-benzothiazolinone hydrazone with hydrogen peroxide. Analytica Chimica Acta 1999;394:55–63.
[20] Ertekin K, Alp S, Karapire C, Yenigül B, Henden E, İçli S. Fluorescence emission studies of an azlactone derivative embedded in polymer films. An optical sensor for pH measurements. Journal of Photochemistry and Photobiology A: Chemistry 2000;137:155–61.
[21] Icli S, Icli H, Koc H, McKillop A. Nmr, absorption and fluorescence parameters of azlactones. Spectroscopy Letters 1994; 27(9):1115–28.
[22] Canet L, Seta P. Extraction and separation of metal cations in solution by supported liquid membrane using lasalocid A as carrier. Pure and Applied Chemistry 2001;73(12):2039–46.